Available online at www.sciencedirect.com
ScienceDirect
Polymer 49 (2008) 635–641
polymer
www.elsevier.com/locate/polymer

# Calculations of the energy of mixing carbon nanotubes with polymers☆

Marc R. Nyden [a,*], Stanislav I. Stoliarov [b]

[a] National Institute of Standards and Technology, Building and Fire Research Laboratory, 100 Bureau Drive, Gaithersburg, MD 20899, United States
[b] SRA International, Egg Harbor Township, NJ 08234, United States

Received 20 September 2007; received in revised form 29 November 2007; accepted 30 November 2007
Available online 8 December 2007

**Abstract**

A method for calculating the energy of mixing carbon nanotubes (CNTs) with polymers is presented. The formation of the nanocomposite is analyzed in terms of a simple path in which the nanotubes are exfoliated from a bundle and dispersed in a distorted polymer with cylindrical cavities to accommodate the nanotubes. From this perspective, the energy of mixing is the difference between the energy required to exfoliate the nanotubes from a bundle and the energy needed to extract the nanotubes from the polymer matrix relative to the relaxed polymer without any nanotubes. These energy components are evaluated by performing molecular mechanics calculations on individual, localized models representing the polymer, nanotube bundles, and polymer/CNT agglomerates. This method is applied to polystyrene/CNT composites and the factors that determine their thermodynamic stability are identified. To a first approximation, the interaction energies (per unit surface area of the nanotubes) are independent of the lengths and chiral indices, but dependent on the diameters of the component nanotubes. By the application of this method, we show that the energy of mixing CNTs with PS is endothermic until the diameters of the component nanotubes exceed about 2.2 nm; at diameters greater than this value the energy of mixing becomes exothermic. This may explain why it is so difficult to obtain good dispersion of single-walled CNTs (SWCNTs) in PS, since they rarely grow to have diameters greater than about 1.4 nm. On the other hand, since the diameters of multi-walled CNTs typically exceed 10 nm, we would expect them to disperse much better than SWCNTs in polystyrene.
Published by Elsevier Ltd.

*Keywords:* Energy of mixing; Molecular mechanics; Nanocomposites

## 1. Introduction

It has been demonstrated that the addition of small quantities of carbon nanotubes (CNTs) can improve the thermal and mechanical properties of polymers [1–7]. In many cases, however, this property enhancement is limited by the degree to which the CNTs can be uniformly dispersed within the polymer matrix [8]. Unfortunately, CNTs are difficult to disperse in most polymers and the composite materials made by mixing them are typically colloidal suspensions, which have a tendency to phase-separate over time. Thus, the properties of these materials may deteriorate with use even when good initial dispersion is achieved by employing high shear mixing techniques. At the source of the problem are the very properties from which the benefits of CNTs derive. More specifically, CNTs reinforce the polymer matrix because they are inherently more rigid and less mobile than the polymer molecules they replace, but these attributes may also limit their miscibility.

In this paper, we continue the development of a simple methodology based on molecular mechanics that can be used to calculate the energy of mixing nanotubes with polymers [9]. Although molecular mechanics has been employed extensively in the past to investigate the structures and mechanical properties of CNTs and polymers, [10–14] its application to the problem of predicting the miscibility of CNTs in polymers is still relatively unexplored with the exception of a paper by Maiti et al. [15]. These authors used molecular mechanics to calculate the cohesive energy densities of nanotube

☆ This article is a US Government work and as such, is in the public domain in the United States of America.

* Corresponding author. +1 301 975 6692.
*E-mail address:* marc.nyden@nist.gov (M.R. Nyden).

0032-3861/$ - see front matter Published by Elsevier Ltd.
doi:10.1016/j.polymer.2007.11.056

bundles as a function of their diameters, from which they obtained the corresponding Hildebrand solubility parameters. By comparing these to accepted values of the solubility parameters for a series of polymers, they were able to make predictions about the diameters required for miscibility. It should be noted, however, that their analysis was based on the Flory–Huggins theory for regular solutions [16]. In our approach, the interactions between CNTs and the polymer are explicitly considered so that changes in coordination that can result in an exothermic enthalpy of mixing are taken into account.

## 2. Description of method

The increase in entropy that accompanies the formation of a mixture is an important factor in determining the miscibilities of small molecules. However, standard treatments of polymer miscibility based on Flory–Huggins theory [17] suggest that the entropies of mixing should be smaller in magnitude for large, immobile molecules, such as CNTs and polymers. This inference follows from the observation that the number of lattice configurations (microstates) representing the mixture will be reduced as a result of constraints imposed by the bonds between the component monomers (and nanotube segments). Thus, assuming that Flory–Huggins theory applies to mixtures of CNTs and polymers, the combinatorial entropy of mixing should fall-off like (molecular weight)$^{-1}$ and, therefore, should become negligible with respect to the enthalpic contribution for sufficiently large CNTs and polymers. Although it is possible that the local ordering of the polymer in the vicinity of the CNTs (resulting in a negative contribution to the entropy of mixing) may actually be more important than the combinatorial effects (which make a positive contribution to the entropy of mixing) addressed in Flory–Huggins theory, this effect should be relatively insensitive to the structures (diameter and chirality) of the component nanotubes. Thus, it should be possible to predict trends in the thermodynamic stability of nanocomposites directly from their enthalpies of mixing ($\Delta H_{\mathrm{mix}}$). Furthermore, the volume change accompanying the formation of the nanocomposite should also be small implying that $\Delta H_{\mathrm{mix}} \approx \Delta E_{\mathrm{mix}}$.

Unfortunately, an explicit calculation of the energy of mixing ($\Delta E_{\mathrm{mix}}$) of polymer/CNT nanocomposites is precluded because of the computational demands involved in evaluating all of the interactions between the atoms, which might contain nanotubes many microns in length and as many as 1000 carbon atoms in the polymer for every carbon atom in the nanotubes (i.e., a loading of $\sim$0.1%). To overcome this limitation we have adopted an approach that makes use of localized molecular models of the polymer, nanocomposite, and nanotubes to estimate the magnitudes of the energies associated with the polymer–polymer (pp), CNT–CNT (nn) and CNT–polymer (np) interactions. The energy of mixing is then evaluated in terms of a simple path in which the nanotubes are exfoliated from a bundle and dispersed in a distorted polymer with cylindrical cavities to accommodate the nanotubes. From this perspective, the energy of mixing is the difference between the energy required to exfoliate the nanotubes from a bundle and the energy needed to extract the nanotubes from the polymer matrix relative to the relaxed polymer without any nanotubes.

Following the logic of this scheme, the energy of mixing can be evaluated from

$$\Delta E_{\mathrm{mix}} = \lfloor \Delta E^{S}_{\mathrm{nn}} - (\Delta E^{S}_{\mathrm{np}} - \Delta E^{S}_{\mathrm{pp}}) \rfloor \times S, \tag{1}$$

where

$$\Delta E^{S}_{\mathrm{nn}} = \frac{\Delta E_{\mathrm{nn}}}{S_n},\ \Delta E^{S}_{\mathrm{np}} = \frac{\Delta E_{\mathrm{np}}}{S_n},\ \Delta E^{S}_{\mathrm{pp}} = \frac{\Delta E_{\mathrm{pp}}}{S_n} \tag{2}$$

are calculated from the energy differences of the model reactions depicted in Fig. 1. The individual terms in Eq. (2) are normalized by dividing by the surface area of the model nanotubes, $S_n$, to facilitate the extrapolation of the results obtained from the atomic length scales of the molecular models to the much larger dimensions that prevail in real materials (i.e., moles of atoms). Thus, as indicated in Eq. (1), the sum of these component energies is multiplied by the total surface area of all of the nanotubes in the nanocomposite, $S$ (obtained as the product of number of nanotubes and the average surface area per nanotube) to calculate the energy of mixing for the experimental material.

In these equations, $\Delta E_{\mathrm{nn}}$ is the energy required to remove a nanotube from a bundle. The magnitude of this term reflects the strength of the interaction between nanotubes. In this study, values for these contributions were obtained by subtracting the energy of a bundle (consisting of 7 CNTs) from that of the smaller bundle where (any) one of the peripheral nanotubes was removed and positioned sufficiently far away so that its interaction with the others was effectively zero. The second term, $\Delta E_{\mathrm{np}}$, is the energy needed to extract a nanotube from a polymer/CNT agglomerate that represents the environment of the nanocomposite in the vicinity of the nanotube. This term accounts for the interactions between the nanotube and polymer. These values were obtained by subtracting the energy of the polymer/CNT agglomerate from that of the structure consisting of the polymer with a cylindrical cavity (where the nanotube was removed) and a noninteracting CNT (i.e., located far enough away that its interaction with the polymer was insignificant). The last term, $\Delta E_{\mathrm{pp}}$, is the energy lowering that results from closing the cylindrical cavity created by the nanotube in the polymer/CNT agglomerate, which should be proportional to the surface energy of the polymer. These values were obtained by multiplying the surface energy of the polymer by the surface area of the cylindrical cavity. The surface area of this cavity is $2\pi(R + d)l$, where $R$ is the radius of the CNT, $l$ is its length, and $d$ is the average distance between the polymer and the surface of the nanotube.

## 3. Computational procedures

Molecular mechanics calculations were performed on models of polystyrene (PS), PS/CNT nanocomposites, and

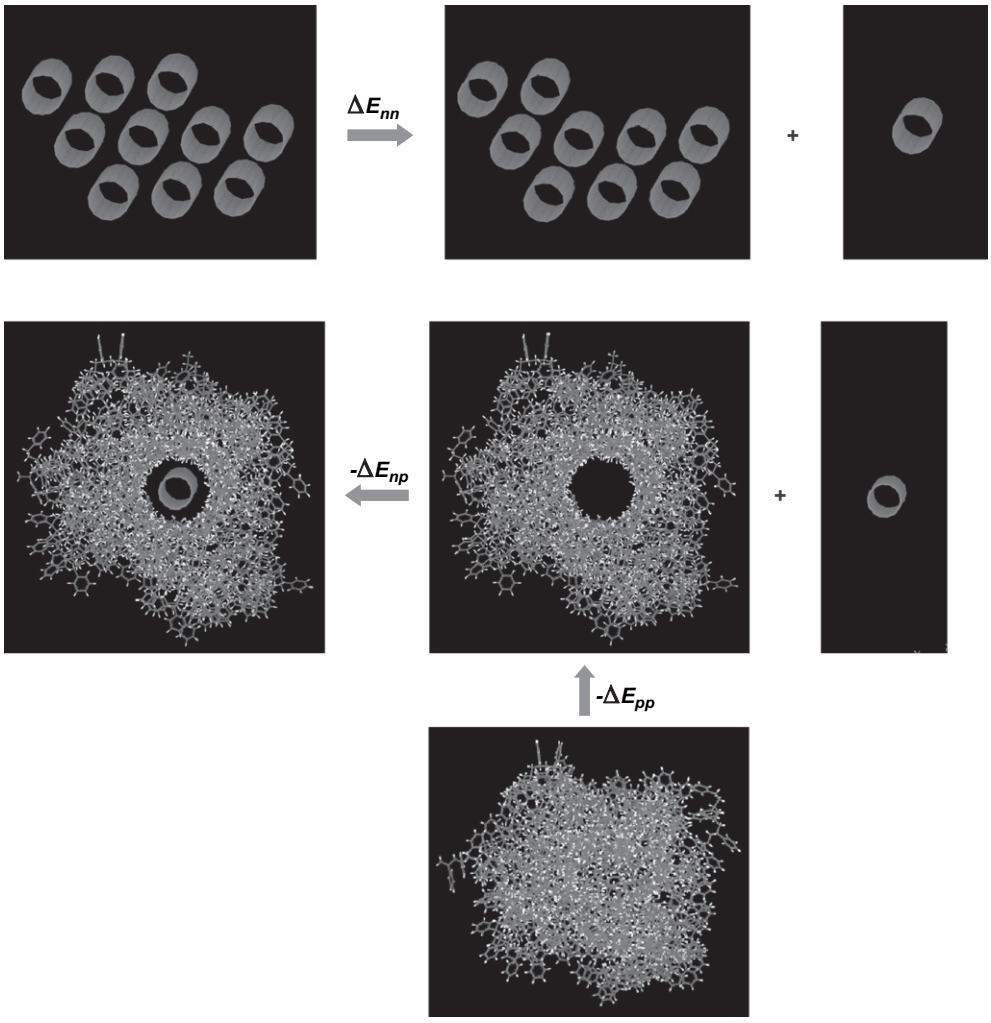


Fig. 1. Processes involved in the formation of a PS/CNT composite from a nanotube bundle and polymer.

nanotube bundles using commercial software package (Hyperchem version 7)[1] with the MM+ force field [18]. Energy optimized structures were determined by employing the Polak–Ribiere conjugate gradient algorithm with an exponential-6 potential (without a cut-off) to represent the nonbonding interactions. Since molecular mechanics calculations consist of minimizing the potential energy without consideration of kinetic energy, they cannot account for the effects of temperature. Thus, we must assume that the relationships between the energy of mixing and nanotube structure, which are derived on the basis of molecular mechanics, are insensitive to temperature.

Calculations of the cohesive energy of graphite and the surface energy of PS were preformed to evaluate the accuracy of the $MM^{+}$ force field and determine its suitability for application to polymer/CNT composites. A model of graphite was constructed by minimizing the energy of a stack consisting of 3 (identical) graphene sheets (3.93 nm × 2.38 nm). The energy of this model was subtracted from that of a second model consisting of 2 graphene sheets with the third sheet separated to "infinity," as described above with respect to the CNT models. After dividing this difference by the area of a single side of the graphene sheet ($A = 9.4\ \mathrm{nm}^2$), we obtained 164 kJ mol$^{-1}$ nm$^{-2}$, which is in close agreement with the accepted experimental value (160 kJ mol$^{-1}$ nm$^{-2}$) for the cohesive energy of graphite [19]. The convergence of the calculated value was examined by repeating these calculations with additional graphene sheets. The effect of the fourth sheet was negligible with respect to the estimated uncertainty of the calculations, ~5%. The surface energy of PS was calculated as follows. A rectangular slab of polymer, with dimensions similar to the graphene sheets, was constructed by stacking 2 layers of PS each consisting of 4 (18 monomer) parallel chains. A second, identical slab was obtained by replicating this structure. The two slabs were then placed on top of each other and a relaxed structure for the bulk assembly was obtained by minimizing its energy. Finally, the surface energy was obtained by dividing the energy required to separate the two component slabs (until their interaction was effectively zero) by the surface area created by their separation ($2A$). The value obtained in this way was $\gamma_{pp} = 39.6$ kJ mol$^{-1}$ nm$^{-2}$, which is in good agreement with

[1] Certain commercial equipment, instruments, materials or companies are identified in this paper in order to adequately specify the experimental procedure. This in no way implies endorsement or recommendation by NIST.

the estimate obtained from extrapolation of experimental measurements of the surface tension of PS to 0 K (37 kJ mol$^{-1}$ nm$^{-2}$) [20]. Again, the convergence was investigated by considering additional layers of polymer, but the calculated value remained essentially constant after the addition of the second layer to each PS slab. Based on these comparisons, we think that the MM+ force field provides a realistic description of the potential energy interactions that determine the energies of mixing CNTs with PS.

Similar calculations were performed to evaluate the energy of interaction (per unit surface area) between graphene and PS, $\Delta E^S_{gp}$. A slab of PS (constructed as described above) was placed on top of a graphene sheet having the same surface area and an optimized structure for the composite was obtained by minimizing its energy. The value, $\Delta E^S_{gp} = 90.7$ kJ mol$^{-1}$ nm$^{-2}$, was calculated by dividing the amount of energy required to separate the PS slab (until the interaction between them was effectively zero) from the graphene by the surface area of the PS slab/graphene sheet ($A$). The convergence of $\Delta E^S_{gp}$ with respect to the addition of subsequent PS layers was also examined as described above. We found that the value did not change (to within the estimated uncertainty of the calculations) after addition of the second layer of polymer. The energy required to remove the PS slab from a stack consisting of 2 graphene sheets was also calculated in an effort to understand the effect of additional nanotube walls on the CNT–polymer interaction energy. We found that the magnitude of $\Delta E^S_{gp}$ increased about 13% (from 90.7 to 102.3 kJ mol$^{-1}$ nm$^{-2}$) by the addition of second graphene sheet. The effect of adding a third sheet was negligible.

Molecular models of zig-zag, arm-chair, and chiral CNTs with diameters ranging from 0.34 to 1.46 nm were constructed and used to make bundles consisting of 7 CNTs (i.e., a central CNT surrounded by 6 nearest neighbors) arranged in a hexagonal lattice without any twists, bends, entanglements, or other defects. The models of these bundles were optimized to determine the lowest energy geometries and used to calculate values for $\Delta E^S_{nn}$, as described above. The effects of the length of the nanotubes and size of the bundles were examined in a previous study where it was found that the values for $\Delta E^S_{nn}$ were insensitive to changes in the number of nanotubes in the bundle (beyond a minimum of 7) and the lengths of the component nanotubes [9].

A model PS/CNT nanocomposite was constructed for each type of CNT by wrapping it with PS chains consisting of 16 monomers. Chains were added until it was determined that the surface of the nanotube was completely covered by polymer and the resulting structure was energy optimized. Additional calculations were performed on some of the models to ensure that the values for $\Delta E^S_{np}$ were converged with respect to the number of polymer chains and invariant to changes in the lengths of the nanotubes. The average value of the distance of separation between the surface of the CNT and inner surface of the surrounding polymer, $d = 0.35$ nm, was found to be independent of the diameter of the CNTs. Constant temperature molecular dynamics simulations were performed at elevated temperatures (500 K) for several picoseconds on each of these structures followed by an energy optimization to generate three independent structures for each PS/CNT agglomerate. The values of $\Delta E^S_{np}$ obtained in this way varied by approximately 5%. The averages are reported in the following section.

## 4. Results

The approach described above was applied in an attempt to understand the factors that determine the thermodynamic stability of PS/CNT composites. Polystyrene was chosen for the first application because it has aromatic rings, which should interact favorably with CNTs based on the premise that "like dissolves like."

The energies required to remove a CNT from a bundle (per unit surface area of nanotube), $\Delta E^S_{nn}$, are listed in Table 1 and plotted in Fig. 2. The variation of the CNT (surface area normalized) binding energies with radius is well-described by Eq. (3)

$$\Delta E^S_{nn}(R) = \frac{C_{nn}}{\sqrt{R}}, \tag{3}$$

with $C_{nn} = 55.2$ kJ mol$^{-1}$ nm$^{-3/2}$. This function appears to fit the calculated values equally well without regard to the chiral

Table 1
Models of CNT bundles

| Chiral indices | Nanotube radius (nm) | Nanotube length (nm) | Number of nanotubes in the bundle | $\Delta E^S_{nn}$ (kJ mol$^{-1}$ nm$^{-2}$) |
|---|---|---|---|---|
| **3_2** | 0.17 | 3.80 | 7 | 131.9 |
| **6_0** | 0.23 | 3.78 | 7 | 117.3 |
| **5_5** | 0.34 | 3.39 | 7 | 92.7 |
| **6_4** | 0.34 | 3.90 | 7 | 92.2 |
| **10_0** | 0.38 | 3.78 | 7 | 90.7 |
| **7_7** | 0.47 | 3.88 | 7 | 81.9 |
| **10_10** | 0.67 | 3.39 | 7 | 67.7 |
| **12_8** | 0.67 | 3.90 | 7 | 67.6 |
| **20_0** | 0.73 | 3.78 | 7 | 67.4 |

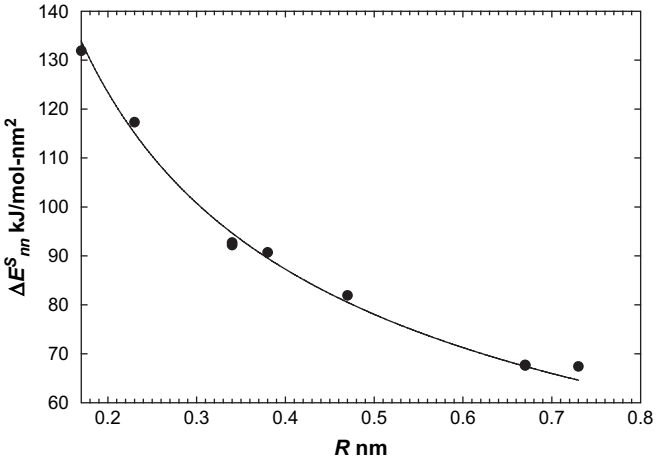


Fig. 2. The values of $\Delta E^S_{nn}$ obtained from MM calculations (points) are well-described by Eq. (3) (line).

indices of the nanotubes (i.e., whether they are zig-zag, arm-chair or chiral).

The observed $R^{-1/2}$ fall-off is consistent with results reported previously by Tersoff and Ruoff [11] and others [12,15]. It arises from the simple fact that the average distance between adjacent cylindrical surfaces (with the same radius) increases from their distance of closest approach with increasing radius. Since the atoms that comprise each of the two interacting nanotubes are on average farther apart in large diameter nanotubes (assuming that their distance of closet approach remains the same), the attraction between them diminishes thereby reducing the cohesive energy per unit surface area of the bundle.

A similar analysis can be applied to both $\Delta E^S_{np}$ and $\Delta E^S_{pp}$. As discussed above, $\Delta E^S_{pp}$ represents the energy lowering (per unit surface area of nanotube) associated with closing the cylindrical cavity occupied by the nanotube and should be proportional to the (negative of the) surface energy of the polymer ($\gamma_{pp} = 39.6$ kJ mol$^{-1}$ nm$^{-2}$). That is,

$$\Delta E^S_{pp}(R) = \frac{-\gamma_{pp} 2\pi (R+d) l}{2\pi R l} = -\gamma_{pp}\left(1+\frac{d}{R}\right). \quad (4)$$

The CNT–polymer interaction energies, $\Delta E^S_{np}$, obtained from our calculations are listed in Table 2 and plotted as a function of CNT radius in Fig. 3. The results are accurately represented by Eq. (5)

$$\Delta E^S_{np}(R) = \Delta E^S_{gp}\left(1+\frac{d}{2R}\right), \quad (5)$$

with $\Delta E^S_{gp} = 90.7$ kJ mol$^{-1}$ nm$^{-2}$ and $d = 0.35$ nm. Here $\Delta E^S_{gp}$ is the energy of interaction between PS and a single graphene sheet (per unit area of graphene) and $d$ is the distance separating the surface of the nanotube from the internal surface of the surrounding polymer (see the discussion in Section 3). The result expressed in Eq. (5) is consistent with the hypothesis that the potential energy of interaction between the CNT and polymer increases in proportion to the sum of the areas of the external surface of the CNT and the internal surface of the surrounding polymer shell. As noted above with respect to the CNT–CNT interaction energies, a single function appears to provide a good representation of the variation of the CNT–polymer interaction energies with $R$, independent of the chiral indices of the nanotubes.

Table 2
Models of PS/CNT agglomerates

| Chiral indices | Nanotube radius (nm) | Nanotube length (nm) | Number of 16-monomer polystyrene chains in the agglomerate | $\Delta E^S_{np}$ (kJ mol$^{-1}$ nm$^{-2}$) |
|---|---|---|---|---|
| **3_2** | 0.17 | 3.80 | 20 | 184.3 |
| **6_0** | 0.23 | 3.78 | 20 | 165.1 |
| **5_5** | 0.34 | 3.39 | 20 | 133.0 |
| **6_4** | 0.34 | 3.90 | 24 | 135.4 |
| **10_0** | 0.38 | 3.78 | 24 | 133.9 |
| **7_7** | 0.47 | 3.88 | 24 | 123.2 |
| **10_10** | 0.67 | 3.39 | 24 | 109.3 |
| **12_8** | 0.67 | 3.90 | 34 | 107.2 |
| **20_0** | 0.73 | 3.78 | 34 | 111.9 |

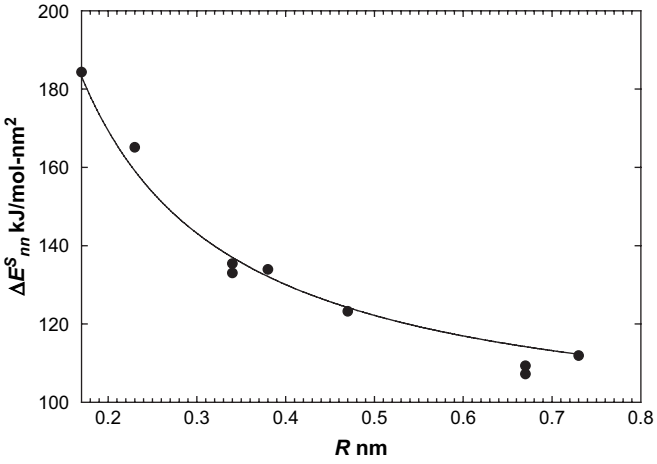


Fig. 3. The values of $\Delta E^S_{np}$ obtained from MM calculations (points) are well-described by Eq. (5) (line).

## 5. Discussion

Substitution of Eqs. (3)–(5) into Eq. (1) results in the following expression for the dependence of the energy of mixing (per unit area) on CNT radius:

$$E^S_{mix}(R) = \Delta E^S_{nn}(R) = \left[\Delta E^S_{np}(R) + \Delta E^S_{pp}(R)\right] = \frac{C_{nn}}{\sqrt{R}} - \left[\left(E^S_{gp} - \gamma_{pp}\right) + \left(\frac{E^S_{gp}}{2} - \gamma_{pp}\right)\frac{d}{R}\right]. \quad (6)$$

The first term on the right hand side of Eq. (6) represents the energy required to remove a single CNT from a bundle. The second term (in brackets) represents the energy needed to extract the same CNT from the polymer matrix; or equivalently, it is the energy released when the CNT dissolves in the polymer matrix. These terms are plotted separately in Fig. 4. The solvation energy initially fall-offs like $R^{-1}$ and

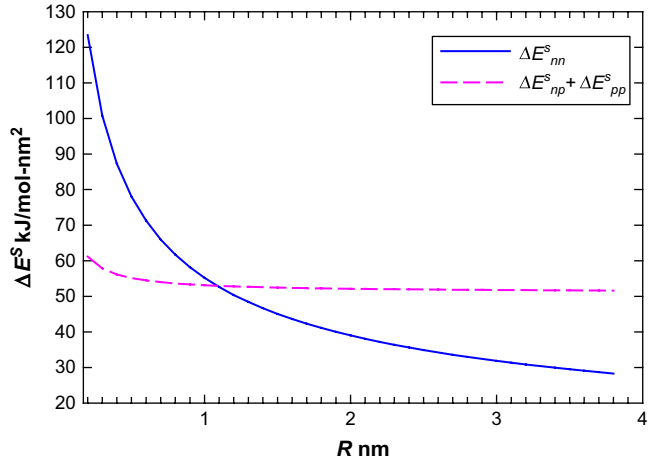


Fig. 4. Plots of the CNT exfoliation (solid line) and solvation (dashed line) energies indicating the radius at which the mixing between CNTS and PS becomes exothermic.

approaches a constant value as $R \to \infty$. This is because the term in the solvation energy that depends on $R^{-1}$ arises from the difference in the areas of the interacting surfaces (i.e., the outer surface of the CNT has less area than the inner surface of the surrounding polymer), which becomes negligible for $R$ greater than about $2d$. The exfoliation energy, which dominates the energy of mixing at small values of $R$ (where $\Delta E_{\mathrm{mix}}$ is endothermic), intersects the curve describing the solvation energy at about $R = 1.1$ nm; after which the energy of mixing becomes exothermic. This intersection occurs after the solvation energy has effectively reached its asymptotic value. Thus, to a good approximation, the critical radius where the energy required to exfoliate a CNT becomes equal to the energy released when it dissolves in the polymer is given by

$$R = \left[\frac{C_{\mathrm{nn}}}{\left(\Delta E^{S}_{\mathrm{gp}} - \gamma_{\mathrm{pp}}\right)}\right]^{2}. \tag{7}$$

On the basis of these calculations, we predict that it should be possible to obtain stable, fully exfoliated nanocomposites by blending CNTs having diameters greater than about 2.2 nm with polystyrene. Since single-walled CNTs (SWCNTs) are typically smaller than this (1.0 nm–1.4 nm in diameter) [21], we conclude that fully exfoliated nanocomposites consisting only of (non-functionalized) SWCNTs and PS are not thermodynamically stable and will have a tendency to agglomerate with the passage of time.

On the other hand, the calculated dependence of $\Delta E_{\mathrm{mix}}$ on nanotube diameter suggests that multi-walled CNTs (MWCNTs), which have diameters ranging from about 10 nm to more than 50 nm, [22] should be completely miscible in PS. This possibility was examined by performing calculations on double-walled nanotubes (DWCNTs). The results indicate that, for DWCNTs, the dependence of $\Delta E^{S}_{\mathrm{nn}}$ on $R$ is well-described by Eq. (3) with $C_{\mathrm{nn}} = 65.5\ \mathrm{kJ\,mol^{-1}\,nm^{-3/2}}$ (i.e., an increase of approximately 19% over the value obtained for SWCNTs) and that the presence of a second sheet of graphene increases the value of $\Delta E^{S}_{\mathrm{gp}}$ from 90.7 to $102.3\ \mathrm{kJ\,mol^{-1}\,nm^{-2}}$ (see discussion in Section 3). Substitution of these values into Eq. (7) gives about the same value ($R = 1.1$ nm) obtained with SWCNTs, suggesting that the critical radius for thermodynamic neutrality is not significantly affected by the presence of the second wall because the increase in $\Delta E^{S}_{\mathrm{nn}}$ is offset by a concomitant increase in $\Delta E^{S}_{\mathrm{gp}}$. Furthermore, the results of our calculations on models consisting of multiple graphene sheets (Section 3) suggest that the inclusion of additional walls (i.e., beyond 2) will not have a significant effect on the values of $\Delta E^{S}_{\mathrm{gp}}$ and $\Delta E^{S}_{\mathrm{nn}}$. Thus, the conclusion that the energy of mixing (non-functionalized) MWCNTs with PS is exothermic appears to be valid.

Another issue that warrants further consideration is the effect of temperature. As discussed in Section 3, the energy differences obtained from our calculations correspond to hypothetical structures at 0 K. Thus, in an effort to obtain a qualitative understanding of how the energy of mixing depends on temperature, we performed a series of constant temperature molecular dynamics simulations on models of CNTs, PS, and PS/graphene composites at temperatures of 100 K, 200 K, and 300 K. From these calculations, it was determined that the CNT exfoliation energy decreases, whereas the solvation energy increases with increasing temperature. Thus, the value of $R$ at which the CNTs become completely miscible in PS, should become smaller with increasing temperature (see Fig. 4). This issue will be examined in greater detail in future investigations.

Our calculations suggest that the thermodynamics of mixing CNTs with polymers becomes more favorable with increasing diameter because the attraction between them (per unit surface area) decreases while the attraction between the CNTs and polymer (per unit surface area) approaches a constant value after an initial, more rapid fall-off (Fig. 4). This difference in behavior is a consequence of the fact that as the diameters of the component CNTs increase, the number of atoms per unit volume in a bundle decreases resulting in a reduction in cohesive energy per atom. On the other hand, the flexibility of the polymer enables it to conform to the spatial constraints that result from the introduction of the CNTs while it maximizes the interactions between the component atoms. The significance of the shape of the nanoadditive on the thermodynamic stability of nanocomposites can be better appreciated when taken in context with the observation that when flat graphene sheets are substituted for CNTs in our calculations, thermodynamic neutrality is never attained. Thus, according to these calculations, the energy of mixing per unit surface area is about $62\ \mathrm{kJ\,mol^{-1}\,nm^{-2}}$ and is independent of the spatial dimensions of the graphene sheet.

## Acknowledgements

The authors would like to acknowledge support received from the Federal Aviation Administration from the Fire Safe Aircraft Cabin Materials Program managed by Dr. Richard Lyon and from an intramural project (monitored by Dr. H. Felix Wu) sponsored by NIST's Advanced Technology Program.

## References

[1] Haggermueller R, Gommans HH, Rinzler AG, Fischer JE, Winey KI. Aligned single-wall carbon nanotubes in composites by melt processing methods. Chem Phys Lett 2000;330:219–25.

[2] Ajayan PM, Schadler LS, Giannaris C, Rubio A. Single-walled carbon nanotube-polymer composites: strength and weakness. Adv Mater 2000; 12:750–3.

[3] Mamedov AA, Kotov NA, Prato M, Guldi DM, Wicksted JP, Hirsch A. Molecular design of strong single-wall carbon nanotube/polyelectrolyte multilayer composites. Nat Mater 2002;1:190–4.

[4] Du F, Fischer JE, Winey KI. Coagulation method for preparing single-walled carbon nanotube/poly(methyl methacrylate) composites and their modulus, electrical conductivity, and thermal stability. J Polym Sci B 2003;4:3333–8.

[5] Ramanathan T, Liu H, Brinson LC. Functionalized SWNT/polymer nanocomposites for dramatic property improvement. J Polym Sci B 2005;43:2269–79.

[6] Bower C, Kleinhammes A, Wu Y, Zhou O. Intercalation and partial exfoliation of single-walled carbon nanotubes by nitric acid. Chem Phys Lett 1998;288:481–6.
[7] Kashiwagi T, Du F, Winey KI, Grotha KM, Shields JR, Bellayer SP, et al. Flammability properties of polymer nanocomposites with single-walled carbon nanotubes: effects of nanotube dispersion and concentration. Polymer 2005;46:471–81.
[8] Kashiwagi T, Fagan J, Yamamoto K, Heckert AN, Leigh SD, Obrzut J, et al. Relationship between quantitative dispersion and physical properties of PMMA/SWNT nanocomposites. Polymer 2007;48:4855–66.
[9] Stoliarov SI, Nyden MR. Molecular mechanics calculations of the thermodynamic stabilities of polymer/carbon nanotube composites. In: Morgan AB, Wilkie CA, editors. Flame retardant polymer nanocomposites. Wiley; 2007.
[10] Robertson DH, Brenner DW, Mintmire JW. Energetics of nanoscale graphitic tubules. Phys Rev B 1992;45:12592–5.
[11] Tersoff J, Ruoff RS. Structural properties of a carbon-nanotube crystal. Phys Rev Lett 1994;73:676–9.
[12] Girifalco LA, Hodak M, Lee RS. Carbon nanotubes, buckyballs, ropes, and a universal graphitic potential. Phys Rev B 2000;62:13104–10.
[13] Gao G, Cagin T, Goddard III WA. Energetics, structure, mechanical and vibrational properties of single-walled carbon nanotubes. Nanotechnology 1998;9:184–91.
[14] Hertel T, Walkup RE, Avouris P. Deformation of carbon nanotubes by surface van der Waals forces. Phys Rev B 1998;58:13870–3.
[15] Maiti A, Wescott J, Kung P. Nanotube-polymer composites: insights from Flory–Huggins theory and mesoscale simulations. Mol Simul 2005;31:143–9.
[16] Hildebrand JH, Scott RL. Regular solutions. Englewood Cliffs, NJ: Prentice Hall; 1962.
[17] Krause S. Polymer–polymer miscibility. Pure Appl Chem 1986;58: 1553–60.
[18] HyperChem(TM) professional 7.52, Hypercube, Inc., 1115 NW 4th Street, Gainesville, Florida 32601, USA.
[19] Girifalco LA, Lad RA. Energy of cohesion, compressibility, and the potential energy functions of the graphite system. J Chem Phys 1956;25:693–7.
[20] Bicerano J. Prediction of polymer properties. 3rd ed. Marcel Dekker; 2002.
[21] Saito Y, Koyama T, Kawabata K. Growth of single-layer carbon tubes assisted with iron-group metal catalysts in carbon arc. Z Phys D 1997;40:421–4.
[22] Ding M, Eitan A, Fisher FT, Chen X, Dikin DA, Andrew R, et al. Direct observation of polymer sheathing in carbon nanotube-polycarbonate composites. Nano Lett 2003;3:1593–7.